JCTC Journal of Chemical Theory and Computation

An Assessment of Density Functional Methods for Potential Energy Curves of Nonbonded Interactions: The XYG3 and B97-D Approximations

Álvaro Vázquez-Mayagoitia,[†] C. David Sherrill,*[,‡] Edoardo Aprà,[§] and Bobby G. Sumpter[§]

Center for Computational Molecular Science and Technology, School of Chemistry and Biochemistry and College of Computing, Georgia Institute of Technology, Atlanta, Georgia 30332-0400, Chemistry Department, University of Tennessee, 1416 Circle Drive, 552 Dabney-Buehler Hall, Knoxville, Tennessee 37996-1600, and Computer Science and Mathematics Division and Center for Nanophase Materials Sciences, Oak Ridge National Laboratory, Bethel Valley Road, P.O. Box 2008, Building 6012, Oak Ridge, Tennessee 37831-6367

Received October 17, 2009

Abstract: A recently proposed double-hybrid functional called XYG3 and a semilocal GGA functional (B97-D) with a semiempirical correction for van der Waals interactions have been applied to study the potential energy curves along the dissociation coordinates of weakly bound pairs of molecules governed by London dispersion and induced dipole forces. Molecules treated in this work were the parallel sandwich, T-shaped, and parallel-displaced benzene dimer, $(C_6H_6)_2$; hydrogen sulfide and benzene, $H_2S \cdot C_6H_6$; methane and benzene, $CH_4 \cdot C_6H_6$; the methane dimer, $(CH_4)_2$; and the pyridine dimer, $(C_5H_5N)_2$. We compared the potential energy curves of these functionals with previously published benchmarks at the coupled cluster singles, doubles, and perturbative triplets [CCSD(T)] complete-basis-set limit. Both functionals, XYG3 and B97-D, exhibited very good performance, reproducing accurate energies for equilibrium distances and a smooth behavior along the dissociation coordinate. Overall, we found an agreement within a few tenths of one kcal mol^{-1} with the CCSD(T) results across the potential energy curves.

I. Introduction

Nonbonded interactions strongly affect protein folding, DNA structure, supramolecular assembly, and drug docking.[1−4] Indeed, any attempt to perform simulations on condensed matter systems is severely handicapped without an adequate description of such interactions. While nonbonded interactions are approximately described by empirical force field methods, these methods are not always accurate for some types of nonbonded interactions, including $\pi-\pi$ stacking.[5] Moreover, even ab initio methods can exhibit significant errors for nonbonded interactions[6−8] unless very large basis sets are used in conjunction with highly correlated methods such as coupled-cluster with perturbative triple excitations, CCSD(T).[9] Unfortunately, most popular density functional approximations completely fail to describe long-range London dispersion interactions.[7,10,11]

Numerous approaches have been advanced to overcome these failures. Of the proposed solutions, the simplest conceptually is to add a damped, empirical dispersion term, yielding a method usually designated as DFT-D.[12−16] This approach seems to give reliable results for nonbonded interactions in a variety of geometries.[17,18] However, while the approach is simple and cost-effective, the use of empirical terms is theoretically unappealing, and the density is not coupled to the dispersion interaction. Other workers have tried reparametrization or extensions of existing types of functionals[19−23] with some success, but ultimately the

* Corresponding author e-mail: sherrill@gatech.edu.
[†] University of Tennessee.
[‡] Georgia Institute of Technology.
[§] Oak Ridge National Laboratory.

10.1021/ct900551z
Published on Web 02/01/2010

physics of long-range dispersion is not captured by local or semilocal functionals.[10] More rigorous approaches include the addition of nonlocal terms to the functional,[24−26] and the exchange dipole moment method of Becke and Johnson.[27−29]

Recently, Zhang, Xu, and Goddard have introduced a "double hybrid" density functional, which mixes in Hartree−Fock exchange as well as contributions from unoccupied orbitals via second-order perturbation theory.[30] Their empirical XYG3 functional uses a scheme of three parameters similar to the B3LYP functional.[31,32] Here, we examine the performance of this double hybrid XYG3 functional for potential energy curves of prototypical nonbonded interactions, and we compare the performance of the XYG3 functional to that of the dispersion-corrected B97-D functional introduced by Grimme.[15] Assessing the quality of these approximations across a range of intermolecular separations is important because, in larger complexes, noncovalent interactions between chemical groups will occur in a wide variety of geometries, and the number of long-range contacts will grow with respect to system size.

II. Theoretical and Computational Details

Density Ffnctional theory (DFT)[33,34] proposes to solve electronic structure problems using as a fundamental variable the electron charge density, $\rho(\vec{r})$; formally, it is based on the Hohenberg and Kohn theorems.[35] In practice, DFT is applied using the Kohn−Sham method (KS), using a mean-field approach.[36] The KS method represents the density as a linear combination of the inner products of spin−orbital functions $\rho(\vec{r}) = \sum_i^{N_{ele}} |\psi_i^{KS}(\vec{r})|^2$, and the energy as a functional of $\rho(\vec{r})$ as

$$E^{DFT}[\rho] = T_0[\rho] + J[\rho] + E_{xc}[\rho] + \int d\vec{r}\, \rho(\vec{r}) v_{ext}(\vec{r}) + V_{NN} \quad (1)$$

where the first and second terms are the kinetic energy of independent particles, $T_0[\rho]$, and the Coulomb interaction energy, $J[\rho] = 1/2 \iint d\vec{r}'\, d\vec{r} \rho(\vec{r}')\rho(\vec{r})/|\vec{r}' - \vec{r}|$. The term $v_{ext}(\vec{r})$ is the external potential generated by the nuclei and felt by the electrons, and V_{NN} is the nuclear repulsion energy for a fixed nuclear configuration. In eq 1, the contribution $E_{xc}[\rho]$ is the exchange-correlation energy, which includes the electron exchange interaction as well as the many-body contribution to the kinetic and electron−electron repulsion potentials ($V_{ee}[\rho]$) that are not included in $T_0[\rho]$ or $J[\rho]$, that is, $E_{xc}[\rho] = V_{ee}[\rho] + T[\rho] - J[\rho] - T_0[\rho]$. The explicit expression of E_{xc} remains unknown, but there are many approaches that have shown satisfactory results. Such approaches have been grouped according to their treatment of the density into "generations" or "ladder's rungs".[37] The most used are based on the Local Density Approximation (LDA) or Generalized Gradient Approximation (GGA).[38] Although some functionals have shown impressive results, those are not totally transferable for every problem and especially fail for the description of long-range interactions and excited states. The origins of these difficulties are attributed to the incorrect cancellation of electron self-interaction,[39] and incorrect treatment of dynamic correlation, among others. There are many strategies to avoid these problems, some of which involve the inclusion of explicit terms from wave function theories (hybrid functionals),[31,40] treatments with optimized effective potentials,[41−43] an adjustment to the asymptotic correction exchange correlation potentials,[44] and the addition of empirical energy terms.

A. Double Hybrid Functionals. The (double) hybrid functionals emerge from the adiabatic connection formalism[31,45] where the exchange correlation functional is obtained solving the follow equation:

$$E_{xc} = \int_0^1 d\lambda\, U_{xc}^{\lambda} \quad (2)$$

The integrand $U_{xc}^{\lambda}[\rho]$ is an exchange-correlation potential energy, keeping fixed the $v_{ext}(\vec{r})$ and $\rho(\vec{r})$ of the physical system, and depending on a dimensionless interelectronic coupling-strength constant, λ, that switches smoothly between a model of independent particles and one of interacting particles around an interval $0 \le \lambda \le 1$, using the KS orbitals as the reference system.

The integrand of eq 2 can be expressed as $U_{xc}^{\lambda} = V_{ee}^{\lambda}[\rho] - J[\rho] + T^{\lambda}[\rho] - T_0[\rho]$; thus this potential depends on λ by virtue of the Hellmann−Feyman theorem. Independently of the form of U_{xc}^{λ}, it is possible to establish certain boundary conditions. The lower integral limit represents the exact exchange, $U_{xc}^{\lambda=0} = V_{ee}^{\lambda=0}[\rho] - J[\rho] + T^{\lambda=0}[\rho] - T_0[\rho] = E_x$, and its upper limit $U_{xc}^{\lambda=1} = V_{ee}^{\lambda=1}[\rho] - J[\rho] + T^{\lambda=1}[\rho] - T_0[\rho] = E_{xc}$, which could be one of the LDA or GGA exchange-correlation energies represented by $U_{xc}^{\lambda=1}[\rho] \approx E_{xc}^{DFT}[\rho]$.

Alternatively, invoking the perturbation scheme proposed by Görling and Levy (GLPT),[46,47] the correlation energy is expanded in a power series around $\lambda = 0$. The first order corresponds to E_x and the second as E_c^{GLPT}; in this formulation, the gradient at $\lambda = 0$ is equal to $(\partial U_{xc}^{\lambda}/\partial\lambda)_{\lambda=0} = 2E_c^{GLPT}$. The E_c^{GLPT} correlation functional explicitly includes single and double orbital transitions, written in Mulliken notation for the electron repulsion integrals as

$$E_c^{GLPT} = -\sum_{ai} \frac{\left|\langle a|\hat{v}_x|i\rangle - \sum_j (aj|ij)\right|^2}{\varepsilon_a - \varepsilon_i} - \frac{1}{4}\sum_{ijab} \frac{[(ia|jb) - (ib|ja)]^2}{\varepsilon_a + \varepsilon_b - \varepsilon_i - \varepsilon_j} \quad (3)$$

where i, j are defined as occupied and a, b as unoccupied KS orbitals, and the exchange potential as $\hat{v}_x = (\delta E_x^{DFT}[\rho]/\delta\rho)$.

Using a first-order interpolator pathway,[48] the integrand in eq 2 can be written as

$$U_{xc}^{\lambda} = a + b\lambda \quad (4)$$

To conciliate the boundary conditions and the correlation formulated by GLPT, an ansatz is used with the parametrical combination of the energy E_c^{GLPT} and E_{xc}^{DFT} within the LDA or GGA exchange-correlation functionals, so the constant b in eq 4 is split into two parameters for the correlation, where the final equation is given by

$$E_{xc} = a_x E_x^{HF} + (1 - a_x)E_x^{DFT} + b_1 E_c^{PT2} + b_2 E_c^{DFT} \quad (5)$$

The term E_c^{PT2} is the correlation energy established from the Møller−Plesset second-order perturbation theory, related to second term in eq 3. The single excitations of E_c^{GLPT} are neglected or simply absorbed by E_c^{DFT}.

The functionals like eq 5 are considered as a last generation and are known as double-hybrid functionals, mainly due to their direct dependence on the occupied and virtual KS orbitals, which offer a way to include the dynamic correlation explicitly, and were originally proposed by Grimme within his B2PLYP functional.[49] The potential generated by the E_c^{GLPT} term acts as a multiplicative operator and can be inserted into the mean-field equation solution via the exchange correlation potential ($\hat{v}_{xc}^{GLPT} = \delta E_{xc}^{GLPT}[\rho]/\delta\rho$) using an optimized effective potential scheme (OEP).[50−53] However, in practice, the orbitals that are used to evaluate the E_c^{PT2} typically come from a mean-field procedure that minimizes the energy for the rest of terms in eq 5.

Zhang, Xu, and Goddard have proposed[30] a set of empirical parameters for a double-hybrid functional called XYG3.

$$E_{xc}^{XYG3} = a_x E_x^{HF} + (1 - a_x)E_x^{Slater} + a_0 \Delta E_x^{B88} + a_c E_c^{PT2} + (1 - a_c)E_c^{LYP} \quad (6)$$

In this case, they adopt the three empirical terms $a_x = 0.8033$, $a_0 = 0.2107$, and $a_c = 0.3211$ in the same spirit as the B3LYP functional, with values that best fit thermodynamical data for the G3/99 set.[54] The functionals E_x^{B88} and E_c^{LYP} denote an exchange functional by Becke[55] and a correlation by Lee, Yang, and Parr, respectively.[56] The main difference with respect to other reparametrizations such as B2K-PLYP,[57] B2GP-PLYP,[58] or B2-P3LYP,[59] which also can produce thermodynamical data and reactions barriers quite similar to those from high-level methods, is that the XYG3 functional adjusts the gradient correction using the parameter a_0 in eq 6, adding the E_x^{Slater} exchange. The XYG3 functional has been tested using the electron density and orbital functions from B3LYP, and this approximation is already capable of accurately reproducing heats of formation, energy barriers, and noncovalent interactions with very good results, and as shown below it can reproduce potential energy surfaces of weak interactions. Although we focus on the XYG3 double hybrid functional in this work, we also discuss limited results for the original B2PLYP double hybrid[49] as well as its empirically corrected variant, B2PLYP-D.[60]

B. Semiempirical Dispersion Contribution. Standard density functionals are local or at best semilocal, and hence they neglect long-range electron correlations, which give rise to attractive London dispersion forces. It has been proposed to simply add an empirical term to account for the missing dispersion energies, that is,

$$E_{DFT\text{-}D} = E^{DFT} + E_{dispersion} \quad (7)$$

From observations, is well-known that the dispersion energy contributes asymptotically to the potential energy in long-range interactions as $U_{disp} \approx -R^{-6}$.[61] Thus, modeling of the dispersion energy as the interaction between pairs of atoms was proposed:[12−16]

$$E_{dispersion} = -s_6 \sum_{i=1}^{N_{at}} \sum_{j>i}^{N_{at}} f(R_{ij}) \frac{C_6^{ij}}{R_{ij}^6} \quad (8)$$

Here, the function $f(R_{ij})$ acts as a damping function, with a gradual transition around a scaled distance R_{ij}^0, which is the sum of individual atomic van der Waals radii, $R_i^0 + R_j^0$. This function is modeled as a Fermi−Dirac-like distribution, $f(R_{ij}) = \{1 + \exp[-\alpha(R_{ij}/R_{ij}^0 - 1])\}^{-1}$, under the control of a global α parameter. The scalar s_6 value in eq 8 weights the whole contribution and is adjusted parametrically for each E_{xc}^{DFT} functional. Furthermore, C_6^{ij} can be determined by an average between the C_6 of i, j atoms, frequently using a geometric mean, $C_6^{ij} = \sqrt{(C_6^i C_6^j)}$.

In this work, we use the E_{xc} proposed by Grimme[15] known as B97-D. This functional is based on a previous one proposed by Becke.[62] Essentially B97-D is a reparametrization to coefficients of an expansion series with a gradient correction factor inside a E_{xc}^{GGA}. The coefficients are optimized by a least-squares fitting procedure, including the term in eq 8, to best reproduce heats of formation from the G2/97 set[63,64] and other properties such as ionization potentials, atomization energies, etc. Additionally, the B97-D functional also attempts to improve the short-range description and avoid the double-counting of electron correlation at medium range distances when the dispersion correction is present. Finally, a remarkable point is that B97-D does not have the E_x^{HF} energy as B97 does, which allows a significant reduction in computational effort, especially when using auxiliary fitted basis functions[65] to evaluate the two-electron integrals.

C. Computational Methods. Computations employed the triple-ζ basis sets used during the development of the functionals considered, TZV2P for B97-D and 6-311+G(3df,2p) for XYG3. We anticipate that the functionals will work best when paired with these basis sets, which were used during their parametrization. Limited tests indicate that the B97-D results are fairly insensitive to basis set, and we found very similar results when using the TZV2P basis or Dunning's aug-cc-pVTZ basis.[66] Earlier work indicates that the typical DFT-D methods are also rather insensitive to basis set superposition error,[15] making counterpoise correction[67] unnecessary. Our results here are not counterpoise corrected unless otherwise noted. The double-hybrid functionals are somewhat more sensitive to basis set and exhibit larger basis set superposition errors because of the perturbation theory term, as we discuss in more detail below.

Both functionals were implemented into the quantum chemistry code NWChem.[68] For the XYG3 functional, we used for the second-order perturbation part the KS orbitals that minimize the energy of the B3LYP functional. For comparison purposes, some results are also obtained using counterpoise-corrected second-order Møller−Plesset perturbation theory (MP2) with an aug-cc-pVDZ basis.

Potential energy curves are evaluated for several prototype dimers for which high-accuracy estimates quantum mechanical benchmarks are available. The benchmark data were obtained by extrapolating MP2 to the complete-basis-set

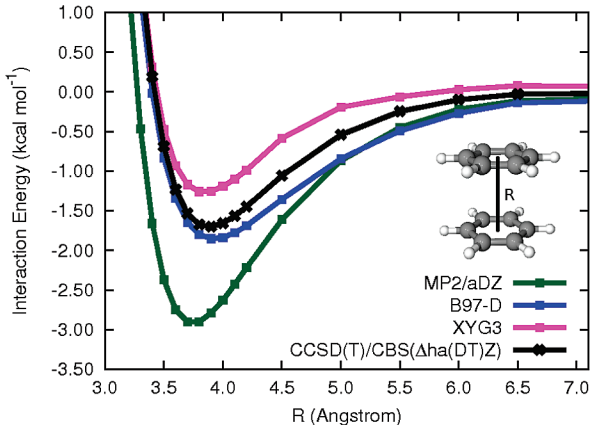

Figure 1. Potential energy curves for the sandwich benzene dimer. CCSD(T)/CBS results from ref 18.

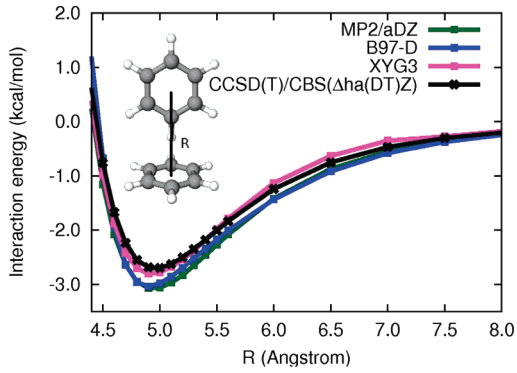

Figure 2. Potential energy curves for the T-shaped benzene dimer. CCSD(T)/CBS results from ref 18.

(CBS) limit, and adding a higher-order electron correlation correction evaluated as the difference between CCSD(T) and MP2 using smaller basis sets. We will denote the basis set(s) used for this "ΔCCSD(T)" correction in parentheses, so that, for example, CCSD(T)/CBS(Δha(DT)Z) denotes an estimate obtained from MP2/CBS binding energies, with a ΔCCSD(T) correction evaluated as the difference between CCSD(T) and MP2, both extrapolated to the CBS limit using a heavy-aug-cc-pVDZ/heavy-aug-cc-pVTZ two-point extrapolation[69] (and where "heavy-aug" indicates only non-hydrogen atoms are augmented by diffuse functions). Recent work indicates that such approximation schemes are very effective at approaching the true CCSD(T)/CBS limit, especially when it is possible to use basis sets larger than augmented double-ζ for the ΔCCSD(T) correction.[18]

Here, we use previously published CCSD(T)/CBS estimates as benchmarks for the following systems: the sandwich, T-shaped, and parallel-displaced configurations of the benzene dimer,[18] methane dimer,[70] methane-benzene,[18] H_2S−benzene,[18] the antiparallel sandwich pyridine dimer,[71] and a T-shaped pyridine dimer.[71]

III. Results and Discussion

Potential energy curves (relative to infinitely separated monomers) are presented in Figures 1−10 for B97-D, XYG3, and estimated CCSD(T)/CBS. The benzene dimer figures also include (counterpoise corrected) MP2/aug-cc-pVDZ results for comparison. Table 1 presents the benchmark

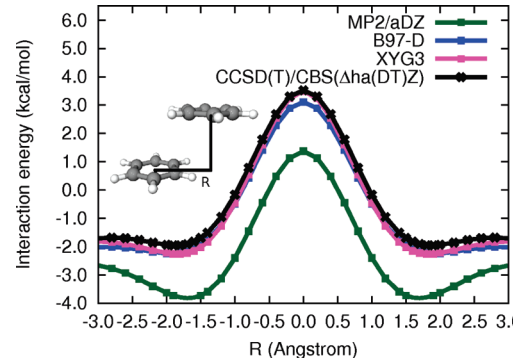

Figure 3. Potential energy curves for the parallel-displaced benzene dimer, with a vertical separation of 3.2 Å. CCSD(T)/CBS results from ref 18.

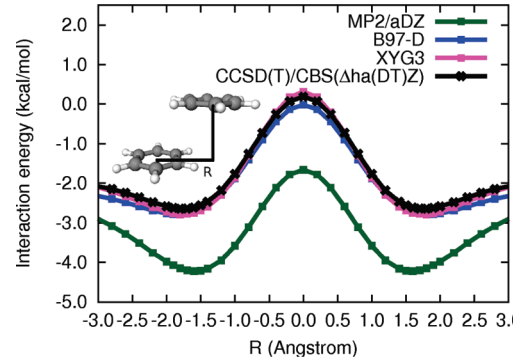

Figure 4. Potential energy curves for the parallel-displaced benzene dimer, with a vertical separation of 3.4 Å. CCSD(T)/CBS results from ref 18.

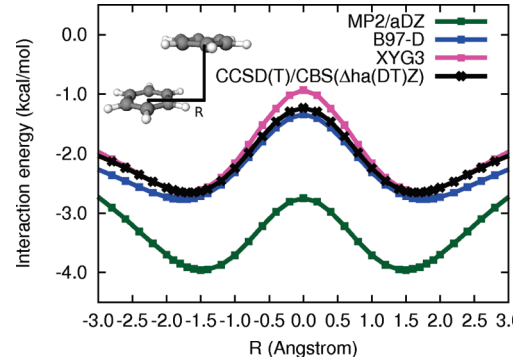

Figure 5. Potential energy curves for the parallel-displaced benzene dimer, with a vertical separation of 3.6 Å. CCSD(T)/CBS results from ref 18.

CCSD(T)/CBS equilibrium intermolecular distances and interaction energies for each system, and the errors in these quantities for each of the approximate methods considered. In general, both the B97-D and the XYG3 methods yield quantitatively reliable potential energy curves. MP2/aug-cc-pVDZ, by contrast, yields qualitatively correct but quantitatively poor curves, which exhibit significant overbinding for the sandwich and parallel-displaced configurations of the benzene dimer. Larger basis sets lead to even greater overbinding by MP2. Because of these fairly large errors, MP2 results are not displayed for the remaining test cases so that the range of the graphs makes the errors for B97-D and XYG3 easier to see.

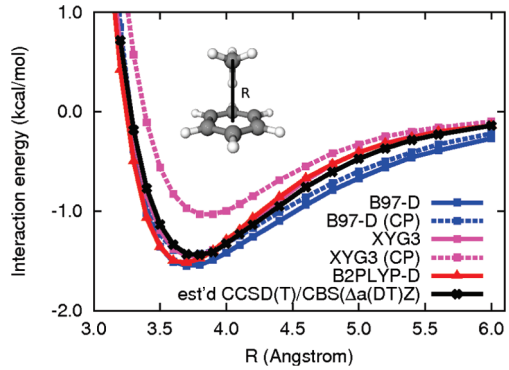

Figure 6. Potential energy curves for the methane−benzene complex. CCSD(T)/CBS results from ref 18. Curves labeled (CP) include counterpoise correction. The XYG3 curve is essentially coincident with the CCSD(T) curve to the left of equilibrium, and coincident with the B2PLYP-D curve to the right of equilibrium.

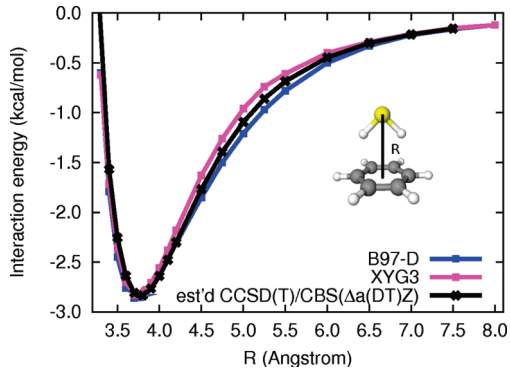

Figure 7. Potential energy curves for the H_2S−benzene complex. CCSD(T)/CBS results from ref 70.

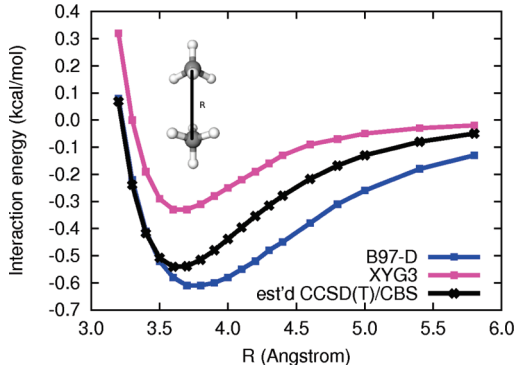

Figure 8. Potential energy curves for the methane dimer. CCSD(T)/CBS results from ref 70.

In the case of the benzene−methane complex (Figure 6), we have examined the effect of counterpoise correction and have compared the XYG3 double hybrid to the B2PLYP-D empirically corrected double hybrid[60] with the TZV2P basis set. We also evaluated the original B2PLYP double hybrid for this case (results not pictured), but B2PLYP-D performs significantly better (the B2PLYP errors are around 0.8 kcal mol^{-1} near equilibrium, as compared to around 0.1 kcal mol^{-1} for B2PLYP-D). For this case, B2PLYP-D and XYG3 are nearly identical. Considering the effect of basis set superposition error, B97-D is hardly affected by counterpoise correction, but the counterpoise-corrected XYG3 curve is significantly underbound and much less accurate than the uncorrected XYG3. This suggests that XYG3 will perform best when used without counterpoise correction and with the 6-311+G(3df,2p) basis set used during its parametrization.

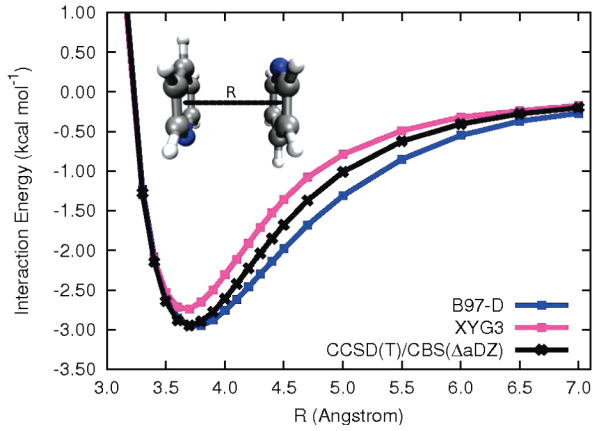

Figure 9. Potential energy curves for the antiparallel sandwich pyridine dimer. CCSD(T)/CBS results from ref 71.

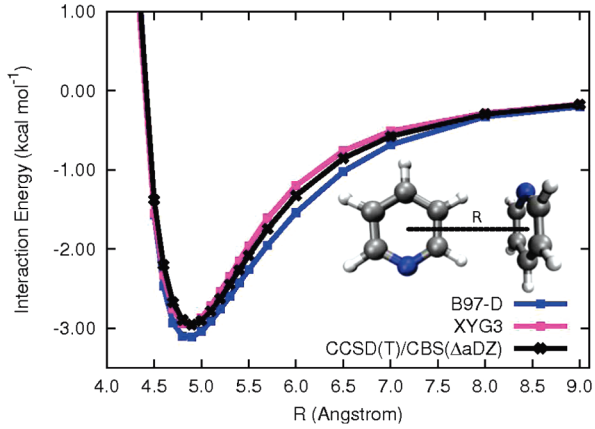

Figure 10. Potential energy curves for a T-shaped pyridine dimer. CCSD(T)/CBS results from ref 71.

Table 1. CCSD(T) Equilibrium Intermolecular Distances (angstroms) and Interaction Energies (kcal mol^{-1}), and Errors for XYG3 and B97-D

	CCSD(T)		XYG3		B97-D	
dimer	R	E_{int}	ΔR	ΔE_{int}	ΔR	ΔE_{int}
benzene dimer sandwich	3.9	−1.701	−0.1	0.443	0.0	−0.151
benzene dimer T-shaped	5.0	−2.698	−0.1	−0.106	−0.1	−0.340
benzene dimer PD (3.2 Å)	1.9	−1.957	0.1	−0.301	0.0	−0.289
benzene dimer PD (3.4 Å)	1.8	−2.643	0.0	−0.147	−0.1	−0.140
benzene dimer PD (3.6 Å)	1.7	−2.654	0.0	−0.002	−0.1	−0.115
CH_4−benzene	3.8	−1.439	−0.1	−0.011	−0.1	−0.111
H_2S−benzene	3.8	−2.834	−0.1	0.004	−0.1	−0.026
CH_4−CH_4	3.6	−0.541	0.0	0.211	0.1	−0.069
pyridine dimer sandwich	3.7	−2.948	0.0	0.208	0.0	−0.002
pyridine dimer T-shaped	4.9	−2.954	0.0	−0.006	0.0	−0.156
mean deviation			0.0	0.029	0.0	−0.140
mean absolute deviation			0.1	0.149	0.1	0.140

For XYG3, the most noticeable errors are for the sandwich benzene dimer and for the methane dimer. In the sandwich benzene dimer, the XYG3 potential well is too shallow by about 0.5 kcal mol^{-1}, and it remains underbound by several tenths of one kcal mol^{-1} at larger distances also. The methane dimer, likewise, is underbound across the potential curve, with errors around 0.2 kcal mol^{-1} near equilibrium; this error decreases slowly as the intermolecular distance increases. These errors are quite small, but they are perhaps significant when compared to the total methane dimer CCSD(T)/CBS interaction energy of −0.54 kcal mol^{-1} at equilibrium. XYG3 shows slight underbinding in the parallel benzene dimer at small horizontal displacements (near the sandwich configuration, amouting to an error of about 0.3 kcal mol^{-1} at a vertical separation of 3.6 Å), and for the antiparallel pyridine sandwich, there is also a slight underestimation of the intermolecular interation (by about 0.2 kcal mol^{-1} near equilibrium). Although somewhat difficult to see from Figure 3, XYG3 is slightly overbound for the parallel-displaced benzene dimer, with errors of around −0.3 kcal mol^{-1} for intermediate horizontal displacements. For the other test cases, the XYG3 potential curves lie very close to the benchmark CCSD(T)/CBS curves. Overall, XYG3 performs very well, with errors of a few tenths of a kcal mol^{-1} or less across the potential curves.

The overall performance of B97-D is quite similar to that of XYG3; it also yields binding energies that are within a few tenths of one kcal mol^{-1} of CCSD(T)/CBS values across the potential curves, but it tends to slightly overestimate binding. B97-D is somewhat more reliable than XYG3 for estimating interaction energies near equilibrium geometries of several of the systems considered here (e.g., sandwich benzene dimer, methane dimer, and the antiparallel sandwich pyridine dimer), but it does not perform as well as XYG3 at the equilibrium geometry of the T-shaped benzene dimer or the T-shaped pyridine dimer. Overall, the mean absolute errors in equilibrium interaction energies are very similar for XYG3 and B97-D (0.15 and 0.14 kcal mol^{-1}, respectively; see Table 1). In a majority of the test cases, B97-D slightly overestimates binding at intermediate to large intermolecular distances.[72] A typical error would be in the range of 0−0.2 kcal mol^{-1}, although it can be larger (e.g., around 0.3 kcal mol^{-1} for the sandwich benzene dimer at an intermolecular separation of 5.0 Å).

Table 2 presents the statistics for the errors across the potential curves considered. Although the more noticeable errors for XYG3 in the figures correspond to a slight underbinding, the mean error across all points considered is actually very close to zero (about 0.01 kcal mol^{-1}). The mean absolute deviation across all points is 0.14, and the maximum error is 0.47 kcal mol^{-1}. As mentioned above, B97-D has a slight tendency to overbind dimers, and this is reflected in the negative mean error in interaction energies of −0.16 kcal mol^{-1}. The mean absolute deviation of 0.18 and the maximum error of 0.68 kcal mol^{-1} are both slightly larger than those observed for XYG3 for the points considered. Overall, then, XYG3 and B97-D appear to perform similarly for these protoypes of nonbonded interactions, with the errors of XYG3 being slightly smaller.

Table 2. Statistics for the Errors of Approximate Methods across the Potential Energy Curves Considered[a]

		XYG3			B97-D		
curve	N_{pts}	MD	MAD	MAX	MD	MAD	MAX
benzene dimer sandwich	17	0.27	0.27	0.47	−0.20	0.20	−0.41
benzene dimer T-shaped	18	−0.05	0.10	−0.24	−0.15	0.22	0.57
benzene dimer PD (3.2 Å)	37	−0.24	0.24	−0.33	−0.32	0.32	−0.41
benzene dimer PD (3.4 Å)	37	−0.07	0.10	−0.15	−0.17	0.17	−0.24
benzene dimer PD (3.6 Å)	37	0.07	0.07	0.30	−0.13	0.13	−0.23
CH_4−benzene	19	0.01	0.04	−0.08	−0.15	0.15	−0.25
H_2S−benzene	19	0.03	0.08	−0.18	−0.06	0.07	−0.22
CH_4−CH_4	18	0.17	0.17	0.25	−0.10	0.10	−0.17
pyridine dimer sandwich	20	0.18	0.20	0.33	−0.12	0.15	−0.31
pyridine dimer T-shaped	19	−0.00	0.10	−0.33	−0.10	0.19	0.68
total	241	0.01	0.14	0.47	−0.16	0.18	0.68

[a] N_{pts} denotes the number of points along the curve. Mean deviation (MD), mean absolute deviation (MAD), and maximum errors (MAX) are given in kcal mol^{-1}.

IV. Conclusions

The recent availability of benchmark-quality potential energy curves for various weakly bound dimers makes it possible to assess the quality of new theoretical methods for describing nonbonded interactions across a range of geometries. Here, we compared the double-hybrid density functional approximation XYG3 and the empirically dispersion-corrected B97-D approach. Both methods performed very well for the potential energy curves considered, with errors no more than a few tenths of one kcal mol^{-1} along the curves. B97-D with its recommended TZV2P basis tends to slightly overbind the dimers considered, while XYG3 with its recommended 6-311+G(3df,2p) basis overbinds about as often as it underbinds. For the benzene−methane complex, we also examined the empirically corrected double-hybrid functional B2PLYP-D,[60] which performed nearly identically to XYG3. For this dimer, we also found that B97-D/TZV2P is rather insensitive to counterpoise correction, whereas counterpoise-corrected XYG3/6-311+G(3df,2p) results were significantly less accurate than the uncorrected values.

The B97-D and XYG3 methods exhibited mean absolute deviations of 0.18 and 0.14 kcal mol^{-1}, respectively, across all geometries considered. Such small errors are difficult to achieve even when using high-level electronic structure methods for these systems,[18] and thus either approach appears to be suitable for typical applications to weakly interacting systems. It should be noted that double-hybrid functionals have a significantly greater computational cost as compared to pure DFT functionals, although in principle this could be alleviated to some extent by using an auxiliary basis and local correlation approaches.

Acknowledgment. We thank Michael S. Marshall for assistance with the figures. This work was supported by the National Science Foundation (Grant No. CHE-0715268) and by the Donors of the American Chemical Society Petroleum Research Fund (Grant No. 44262-AC6). The Center for

Computational Molecular Science and Technology is funded through an NSF CRIF award (CHE 04-43564) and by Georgia Tech. B.G.S. acknowledges support by the Center for Nanophase Materials Sciences (CNMS), sponsored by the Division of Scientific User Facilities, U.S. Department of Energy. E.A. and A.V.M. acknowledge support from the Department of Energy, Offices of Basic Energy Science and Advanced Scientific Computing Research as part of the SciDAC program. This research used resources supported by the Office of Science of the U.S. Department of Energy under Contract No. DE-AC05-00OR22725.

Supporting Information Available: Cartesian coordinates for equilibrium geometries, and potential energy curves of the complexes. This material is available free of charge via the Internet at http://pubs.acs.org.

References

(1) Steed, J. W.; Atwood, J. L. *Supramolecular Chemistry: A Concise Introduction*; Wiley: New York, 2000.

(2) Lehn, J.-M. *Supramolecular Chemistry: Concepts and Perspectives*; VCH: New York, 1995.

(3) Diederich, F., Künzer, H., Eds. *Recent Trends in Molecular Recognition*; Springer: New York, 1998.

(4) Meyer, E. A.; Castellano, R. K.; Diederich, F. *Angew. Chem., Int. Ed.* **2003**, *42*, 1210–1250.

(5) Sherrill, C. D.; Sumpter, B. G.; Sinnokrot, M. O.; Marshall, M. S.; Hohenstein, E. G.; Walker, R. C.; Gould, I. R. *J. Comput. Chem.* **2009**, *30*, 2187–2193.

(6) Hobza, P.; Selzle, H. L.; Schlag, E. W. *J. Phys. Chem.* **1996**, *100*, 18790–18794.

(7) Tsuzuki, S.; Lüthi, H. P. *J. Chem. Phys.* **2001**, *114*, 3949.

(8) Sinnokrot, M. O.; Sherrill, C. D. *J. Phys. Chem. A* **2006**, *110*, 10656–10668.

(9) Raghavachari, K.; Trucks, G. W.; Pople, J. A.; Head-Gordon, M. *Chem. Phys. Lett.* **1989**, *157*, 479–483.

(10) Kristyán, S.; Pulay, P. *Chem. Phys. Lett.* **1994**, *229*, 175–180.

(11) Johnson, E. R.; Wolkow, R. A.; DiLabio, G. A. *Chem. Phys. Lett.* **2004**, *394*, 334–338.

(12) Wu, Q.; Yang, W. *J. Chem. Phys.* **2002**, *116*, 515–524.

(13) Grimme, S. *J. Comput. Chem.* **2004**, *25*, 1463–1473.

(14) Zimmerli, U.; Parrinello, M.; Koumoutsakos, P. *J. Chem. Phys.* **2004**, *120*, 2693.

(15) Grimme, S. *J. Comput. Chem.* **2006**, *27*, 1787–1799.

(16) Jurečka, P.; Černý, J.; Hobza, P.; Salahub, D. R. *J. Comput. Chem.* **2007**, *28*, 555–569.

(17) Hohenstein, E. G.; Chill, S. T.; Sherrill, C. D. *J. Chem. Theory Comput.* **2008**, *4*, 1996–2000.

(18) Sherrill, C. D.; Takatani, T.; Hohenstein, E. G. *J. Phys. Chem. A* **2009**, *113*, 10146–10159.

(19) Xu, X.; Goddard, W. A. *Proc. Natl. Acad. Sci. U.S.A.* **2003**, *101*, 2673–2677.

(20) Zhao, Y.; Schultz, N. E.; Truhlar, D. G. *J. Chem. Phys.* **2005**, *123*, 161103.

(21) Zhao, Y.; Schultz, N. E.; Truhlar, D. G. *J. Chem. Theory Comput.* **2006**, *2*, 364–382.

(22) Zhao, Y.; Truhlar, D. G. *J. Chem. Phys.* **2006**, *125*, 194101.

(23) Zhao, Y.; Truhlar, D. G. *Theor. Chem. Acc.* **2008**, *120*, 215–241.

(24) von Lilienfeld, O. A.; Tavernelli, I.; Rothlisberger, U.; Sebastiani, D. *Phys. Rev. Lett.* **2004**, *93*, 153004–153007.

(25) von Lilienfeld, O. A.; Tavernelli, I.; Rothlisberger, U.; Sebastiani, D. *Phys. Rev. B* **2005**, *71*, 195119.

(26) Dion, M.; Rydberg, H.; Schröder, E.; Langreth, D. C.; Lundqvist, B. I. *Phys. Rev. Lett.* **2004**, *92*, 246401–246404.

(27) Becke, A. D.; Johnson, E. R. *J. Chem. Phys.* **2005**, *123*, 154101.

(28) Johnson, E. R.; Becke, A. D. *J. Chem. Phys.* **2005**, *123*, 024101.

(29) Becke, A. D.; Johnson, E. R. *J. Chem. Phys.* **2006**, *124*, 014104.

(30) Zhang, Y.; Xu, X.; Goddard, W. A. *Proc. Natl. Acad. Sci. U.S.A.* **2009**, *106*, 4963–4968.

(31) Becke, A. D. *J. Chem. Phys.* **1993**, *98*, 1372–1377.

(32) Stephens, P. J.; Devlin, F. J.; Chabalowski, C. F.; Frisch, M. J. *J. Phys. Chem.* **1994**, *98*, 11623–11627.

(33) Parr, R.; Yang, W. *Density Functional Theory of Atoms and Molecules*; Oxford University Press: New York, 1989.

(34) Kohanoff, J. *Electronic Structure Calculations for Solids and Molecules: Theory and Computational Methods*; Cambridge University Press: New York, 2006.

(35) Hohenberg, P.; Kohn, W. *Phys. Rev.* **1964**, *136*, B864–B871.

(36) Kohn, W.; Sham, L. J. *Phys. Rev.* **1965**, *140*, A1133–A1138.

(37) Perdew, J. P.; Schmidt, K. *Jacob's Ladder of Density Functional Approximations for the Exchange-Correlation Energy*; AIP: New York, 2001; Vol. 577.

(38) Perdew, J.; Kurth, S. *A Primer in Density Functional Theory*; Springer Verlag: Berlin Heidelberg, 2003.

(39) Perdew, J. P.; Zunger, A. *Phys. Rev. B* **1981**, *23*, 5048–5079.

(40) Csonka, G.; Johnson, B. *Theor. Chem. Acc.* **1998**, *99*, 158–165.

(41) Krieger, J. B.; Li, Y.; Iafrate, G. J. *Phys. Rev. A* **1992**, *46*, 5453–5458.

(42) Krieger, J.; Li, Y.; Iafrate, G. J. *Phys. Rev. A* **1992**, *45*, 101–126.

(43) Garza, J.; Nichols, J. A.; Dixon, D. A. *J. Chem. Phys.* **2000**, *112*, 7880.

(44) Levy, M.; Perdew, J. P.; Sahni, V. *Phys. Rev. A* **1984**, *30*, 2745–2748.

(45) Frydel, D.; Terilla, W. M.; Burke, K. *J. Chem. Phys.* **2000**, *112*, 5292–5297.

(46) Görling, A.; Levy, M. *Phys. Rev. B* **1993**, *47*, 13105.

(47) Teale, A. M.; Coriani, S.; Helgaker, T. *J. Chem. Phys.* **2009**, *130*, 104111.

(48) Peach, M. J. G.; Miller, A. M.; Teale, A. M.; Tozer, D. J. *J. Chem. Phys.* **2008**, *129*, 064105.

(49) Grimme, S. *J. Chem. Phys.* **2006**, *124*, 034108.

(50) Mori-Sánchez, P.; Wu, Q.; Yang, W. *J. Chem. Phys.* **2005**, *123*, 062204.

(51) Facco Bonetti, A.; Engel, E.; Schmid, R. N.; Dreizler, R. M. *Phys. Rev. Lett* **2001**, *86*, 2241–2244.

(52) Grabowski, I.; Hirata, S.; Ivanov, S.; Bartlett, R. J. *J. Chem. Phys.* **2002**, *116*, 4415–4425.

(53) Kümmel, S.; Kronik, L. *Rev. Mod. Phys.* **2008**, *80*, 3–60.

(54) Curtiss, L. A.; Redfern, P. C.; Raghavachari, K.; Pople, J. A. *Chem. Phys. Lett.* **1999**, *313*, 600–607.

(55) Becke, A. D. *Phys. Rev. A* **1988**, *38*, 3098–3100.

(56) Lee, C.; Yang, W.; Parr, R. G. *Phys. Rev. B* **1988**, *37*, 785–789.

(57) Tarnopolsky, A.; Karton, A.; Sertchook, R.; Vuzman, D.; Martin, J. M. L. *J. Phys. Chem. A* **2008**, *112*, 3–8.

(58) Karton, A.; Tarnopolsky, A.; Lamére, J.-F.; Schatz, G. C.; Martin, J. M. L. *J. Phys. Chem. A* **2008**, *112*, 12868–12886.

(59) Benighaus, T.; DiStasio, R., Jr.; Lochan, R.; Head-Gordon, M. *J. Phys. Chem. A* **2008**, *112*, 2702–2712.

(60) Schwabe, T.; Grimme, S. *Phys. Chem. Chem. Phys.* **2007**, *9*, 3397–3406.

(61) Stone, A. *The Theory of Intermolecular Forces*; Oxford University Press: New York, 1997.

(62) Becke, A. D. *J. Chem. Phys.* **1997**, *107*, 8554–8560.

(63) Curtiss, L. A.; Raghavachari, K.; Redfern, P. C.; Pople, J. A. *J. Chem. Phys.* **1997**, *106*, 1063–1079.

(64) Curtiss, L. A.; Redfern, P. C.; Raghavachari, K.; Pople, J. A. *J. Chem. Phys.* **1998**, *109*, 42–55.

(65) Eichkorn, K.; Treutler, O.; Öhm, H.; Häser, M.; Ahlrichs, R. *Chem. Phys. Lett.* **1995**, *240*, 283–289.

(66) Kendall, R. A.; Dunning, T. H.; Harrison, R. J. *J. Chem. Phys.* **1992**, *96*, 6796.

(67) Boys, S. F.; Bernardi, F. *Mol. Phys.* **1970**, *19*, 553–566.

(68) Bylaska, E. J.; de Jong, W. A.; Govind, N.; Kowalski, K.; Straatsma, T. P.; Valiev, M.; Wang, D.; Apra, E.; Windus, T. L.; Nichols, J. H. P.; Hirata, S.; Hackler, M. T.; Zhao, Y.; Fan, P.-D.; Harrison, R. J.; Dupuis, M.; Smith, D. M. A.; Nieplocha, J.; Tipparaju, V.; Krishnan, M.; Wu, Q.; Voorhis, T. V.; Auer, A. A.; Nooijen, M.; Brown, E.; Cisneros, G.; Fann, G. I.; Fruchtl, H.; Garza, J.; Hirao, K.; Kendall, R.; Nichols, J. A.; Tsemekhman, K.; Wolinski, K.; Anchell, J.; Bernholdt, D.; Borowski, P.; Clark, T.; Clerc, D.; Dachsel, H.; Deegan, M.; Dyall, K.; Elwood, D.; Glendening, E.; Gutowski, M.; Hess, A.; Jaffe, J.; Johnson, B.; Ju, J.; Kobayashi, R.; Kutteh, R.; Lin, Z.; Littlefield, R.; Long, X.; Meng, B.; Nakajima, T.; Niu, S.; Pollack, L.; Rosing, M.; Sandrone, G.; Stave, M.; Taylor, H.; Thomas, G.; van Lenthe, J.; Wong, A.; Zhang, Z. *NWChem, A Computational Chemistry Package for Parallel Computers, version 5.1*; Pacific Northwest National Laboratory: Richland, WA, 2007.

(69) Halkier, A.; Helgaker, T.; Jørgensen, P.; Klopper, W.; Koch, H.; Olsen, J.; Wilson, A. K. *Chem. Phys. Lett.* **1998**, *286*, 243–252.

(70) Takatani, T.; Sherrill, C. D. *Phys. Chem. Chem. Phys.* **2007**, *9*, 6106–6114.

(71) Hohenstein, E. G.; Sherrill, C. D. *J. Phys. Chem. A* **2009**, *113*, 878–886.

(72) Peverati, R.; Baldridge, K. *J. Chem. Theory Comput.* **2008**, *4*, 2030–2048.

CT900551Z